IEEE Access
Multidisciplinary | Rapid Review | Open Access Journal

Received November 21, 2019, accepted December 14, 2019, date of publication December 17, 2019,
date of current version December 27, 2019.

*Digital Object Identifier 10.1109/ACCESS.2019.2960404*

# Analysis of the High-Frequency Response of Thin Wires Irradiated by Electromagnetic Waves Through Tikhonov Regularization Technique

**YIN ZHANG, CHENG LIAO, YUPING SHANG, WEI DU, AND RUI HUAN**
Institute of Electromagnetics, Southwest Jiaotong University, Chengdu 610031, China

Corresponding author: Cheng Liao (c.liao@swjtu.edu.cn)

This work was supported in part by the National Natural Science Foundation of China under Grant 61771407 and Grant 61601379, and in part by the Fundamental Research Funds for the Central Universities under Grant 2682018CX41.

**ABSTRACT** The formula for analyzing the response characteristics of the induced current on a transmission line (TL) excited by high-frequency electromagnetic (EM) waves is a mixed integral-differential equation. The integral part is the Fredholm integral equation of the first kind with serious ill-posedness, which causes difficulty in solving it stably. The regularization technique is a useful method for the analysis of the ill-posed problems. Therefore, in this paper, a method based on the Tikhonov regularization technique is proposed to analyze the high-frequency electromagnetic response of a finite length TL illuminated by external EM waves. The integral operator is discretized by the Simpson formula. The validity and correctness of the proposed method have been verified by numerical examples and the applicability of the proposed method at different errors has been analyzed via the TL with different height.

**INDEX TERMS** Tikhonov regularization technique, mixed integral-differential equation, transmission line, high-frequency electromagnetic response, discretization.

## I. INTRODUCTION

A transmission line (TL) is an important connecting component that carries the function of transmitting signals and energy in modern electronic and electrical equipment. Thin lines can be seen as a type of TL. When the TL is irradiated by an external electromagnetic (EM) waves, the induced voltage/current on the TL may lead to an increase in the error rate of the signal, or cause malfunction in the internal sensitive components, such as semiconductor, and thereby disable the system. Therefore, the response problem of the TL excited by EM waves has always been an important topic in the electromagnetic compatibility field [1], [2].

For the cases where an analysis condition named low-frequency approximation is satisfied or only the induced voltage/current at the terminal loads of the TL is to be studied, the classic TL models are fully capable of fulfilling the requirement [3], [4]. However, with the recent development of high-frequency (HF) electronic and electrical equipment, the threat from high-frequency electromagnetic (HFEM) waves is gradually increasing. In many cases, it is necessary to consider not only the EM response at the terminal loads, but also the scattering effect of the TL itself [5]. The HF field-line coupling problems were studied by introducing HF correction components to the source terms of classic TL equations in 1995 [6]. In the TRI model proposed by Tkatchenko *et al.* in 2001 [7], the TL is divided into three segments to analyze its HFEM response problem, which is very effective for a very long TL. However, a shortcoming of that model is that the analysis of asymptotic segments requires a full-wave simulation. In view of the deficiencies of the TRI model, some more in-depth research was carried on the basis of the TRI model. The generalized TL model and mixed integral-differential equations have been derived and solved by various methods, such as boundary element method [8], product integral method [9], and regularization technique [10], [11]. While the TRI model is gradually improved, the transmission line super theory (TLST) based on Maxwell's equation was proposed [12], [13], and its combination with the BLT equation was realized [14]. Afterwards, the TLST was systematically explained in [15] and its numerical implementation process was also shown in detail in an analysis

The associate editor coordinating the review of this manuscript and approving it for publication was Flavia Grassi.

example of multi-conductor transmission line (MTL) [16]. The enhanced transmission line (ETL) model is also a useful method for the analysis of the response characteristics of the TL irradiated by HFEM waves, but there is a big difference between it and the classic TL model [17].

Based on the literature, it is noted that the response characteristics of the TL illuminated by HFEM waves can be expressed by a mixed integral-differential equation. When the integral part is considered as a whole, the expression can be equivalent to a second-order non-homogeneous differential equation which is very easy to be solved. The integral part belongs to the Fredholm integral equation of the first kind with ill-posedness [18], which means that an unacceptable error may occur in the final result when the observed data at the right of the equation change slightly. For the analysis of ill-posed problems, the regularization technique is a very mature method. In this method, the exact solution is fitted by a regularization solution obtained by adding a penalty term to the original equation. The regularization technique has been applied successfully in the analysis of various inverse problems [19]–[24]. Therefore, the Tikhonov regularization technique is adopted to solve the mixed integral-differential equation and analyze the HFEM response characteristics of the TL in this study.

The remainder of this paper is organized as follows. Section II details the analytical process of solving the integral-differential equation by the Tikhonov regularization technique. The principles of selection of the regularization parameter and discrete points are introduced in Section III. The effectiveness of the proposed method is verified by numerical examples in Section IV. Section V summarizes our work.

## II. ANALYTICAL PROCESS OF THE INTEGRAL-DIFFERENTIAL EQUATION SOLVED BY TIKHONOV REGULARIZATION TECHNIQUE

An overhead TL with finite length locates along the $x$-axis in the homogeneous, isotropic, and loss-free half-space above the ground made of perfectly electrically conductor (PEC), as shown in Fig. 1. We shall analyze the HFEM response of an overhead finite length TL with an open-circuit condition. The length, height, and radius of the TL are $l$, $h$, and $r$, respectively. The EM properties of the medium in $z > 0$ are described by its permittivity $\varepsilon_0$ and permeability $\mu_0$. The propagation direction of the EM waves is $\boldsymbol{K}$ and is defined by the pitch angle $\phi$, azimuth angle $\gamma$, and polarization angle $\theta$.

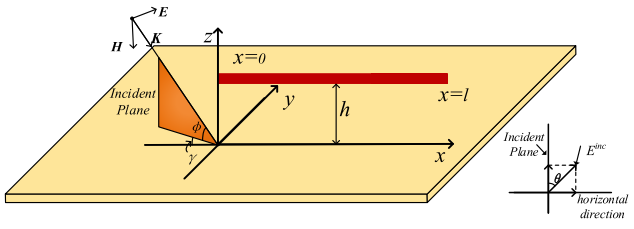


**FIGURE 1.** The overhead single-conductor TL irradiated by an incident plane EM waves.

### A. DERIVATION OF THE MIXED INTEGRAL-DIFFERENTIAL EQUATION

The generalized TL model is briefly derived in this part. PEC is considered as the material of the overhead TL with a finite length and open-circuit terminal condition. It should be pointed out that all the equations are written in the frequency domain and with a time-harmonic dependence $e^{j\omega t}$ for all the variables.

In the Lorenz gauge, the x-component of the vector potential $A(x)$ of the scattered current can be described as follows,

$$A_x(x) = \frac{\mu_0}{4\pi}\int_{-L}^{L} g\left(x-x'\right) I\left(x'\right)\,\mathrm{d}x' \tag{1}$$

A scattering field $E^{\mathrm{sca}}$ can be generated by a conductor irradiated by EM waves. At the surface of the conductor, the tangential components of the incident and scattered electric fields must satisfy the following zero-boundary condition,

$$E_x^{\mathrm{total}}(x) = E_x^{\mathrm{inc}}(x) + E_x^{\mathrm{sca}}(x) = 0 \tag{2}$$

The tangential component of the scattered field is expressed by the tangential components of both the vector and scalar potentials.

$$E_x^{\mathrm{sca}}(x) = -\frac{\mathrm{d}}{\mathrm{d}x}\varphi\left(x\right) - j\omega A_x\left(x\right) \tag{3}$$

Then we use the following connection

$$\frac{\mathrm{d}}{\mathrm{d}x}A_x\left(x\right) + j\frac{\omega}{c_0^2}\varphi\left(x\right) = 0 \tag{4}$$

which relates the vector and scalar potentials in the Lorenz gauge. Together with (2) and (3), the HFEM response model for the induced voltage and current on the overhead TL can be obtained as follows,

$$\left(\frac{\mathrm{d}^2}{\mathrm{d}x^2} + k^2\right)\int_{-L}^{L} g(x-x')I(x')dx' = -\frac{4\pi k^2}{j\omega\mu_0}E_x^{\mathrm{inc}}\left(x\right) \tag{5}$$

where $\omega = 2\pi f$ defines the angular frequency. The $V_s$ is the scattering voltage generated by a TL illuminated by EM waves. The $c_0$ is the speed of light in vacuum. The $k = \omega/c_0$ represents the wavenumber. The $E_x^{\mathrm{inc}}$ is equal to the superposition of the $x$-component of the incident and reflected EM waves. The $g(x-x')$ defines the Green function and can be expressed as follows,

$$g(x-x') = \frac{\mathrm{e}^{-jk\sqrt{r^2+(x-x')^2}}}{\sqrt{r^2+(x-x')^2}} - \frac{\mathrm{e}^{-jk\sqrt{4h^2+(x-x')^2}}}{\sqrt{4h^2+(x-x')^2}} \tag{6}$$

It is noted that (5) is a mixed integral-differential equation. If the integral part of (5) is regarded as a whole and replaced by a coefficient, the equation becomes equivalent to a second-order non-homogeneous differential equation

whose solution general expression can be easily obtained. Therefore, the analysis of the above integral part is the main objective of this work.

The general expression of the solution of (5) is a linear superposition of the results of three Fredholm integral equations of the first kind [10], [11].

$$\int_{-L}^{L} g(x-x')I(x')\,\mathrm{d}x' = C_1 \mathrm{e}^{jkx} + C_2 \mathrm{e}^{-jkx} + T(x) \quad (7)$$

where $C_1$ and $C_2$ are unknown coefficients and $T(x)$ is the particular solution of (5).

It is known that (7) can be rewritten as three equations,

$$\int_{-L}^{L} g(x-x')I_1(x')\,\mathrm{d}x' = \mathrm{e}^{jkx} \quad (8\text{-}1)$$

$$\int_{-L}^{L} g(x-x')I_2(x')\,\mathrm{d}x' = \mathrm{e}^{-jkx} \quad (8\text{-}2)$$

$$\int_{-L}^{L} g(x-x')I_3(x')\,\mathrm{d}x' = T(x) \quad (8\text{-}3)$$

Therefore, the HF induced current studied in this work can be represented by a superposition of three components of the induced current in (8).

$$I(x) = C_1 I_1(x) + C_2 I_2(x) + I_3(x) \quad (9)$$

The last step involves the determination of the coefficients $C_1$ and $C_2$. As shown in Fig. 1, the model is considered with open-circuit condition at the two terminals in this paper. Therefore, the induced currents at the two terminals are $I(-L) = I(L) = 0\mathrm{A}$.

### B. PROCESS OF TIKHONOV REGULARIZATION

Then, the analysis of (8) is carried out. However, the three equations in (8) belong to the Fredholm integral equation of the first kind and are difficult to be solved stably, which means an unacceptable error may occur in the final result when the observed data at the right of the equation change slightly. Unfortunately, in practice, the small changes in the observed data are quite common. For an overhead TL, some small changes in the electric field around it may be caused by the wind, gravity, changes of temperature or undesirable factors in the surrounding environment. In [10], [11], the Landweber iterative regularization technique (LIRT) is adopted to solve the ill-posed equation, but a great number of iterative calculations have to be experienced and a large amount of time spent is necessary before a stable result is obtained. In order to avoid this problem, a Tikhonov regularization technique is adopted in this study to achieve the purpose of solving (8) stably and quickly.

In (8), the properties of (8-1) and (8-2) are the same and their solutions are only related to the configuration of a TL itself, and independent of the influence of incident EM waves. But the induced current is affected by the EM environment in (8-3).

$$\int_{-L}^{L} g(x-x')I(x')\,\mathrm{d}x' = D(x) \quad (10)$$

The Simpson rule is used to discretize the kernel function of (10). Then, the integral expression $\int_{-L}^{L} g(x-x')I(x')\,\mathrm{d}x'$ is replaced by an accumulation formula $\sum_{n=0}^{N} B_n g(x_i - x_n) I(x_n)$. According to the Simpson formula, the coefficients $B$ after discretization can be represented as follow,

$$B_n = \begin{cases} \dfrac{1}{3N}, & n = 0 \text{ or } N \\ \dfrac{4}{3N}, & n = 1, 3, \cdots, N\text{-}1 \\ \dfrac{2}{3N}, & n = 2, 4, \cdots, N\text{-}2 \end{cases} \quad (11)$$

where $N$ defines the number of the discrete points in the integral range $[-l, l]$ and $x = i/N$, at $i = 0, 1, 2, \cdots, N$, the $N$ is even. A matrix is obtained after the discretization.

$$\boldsymbol{A} = \begin{bmatrix} A_{11} & A_{12} & \cdots & A_{1N} \\ A_{21} & A_{22} & \cdots & A_{2N} \\ \cdots & \cdots & \cdots & \cdots \\ A_{N1} & A_{N2} & \cdots & A_{NN} \end{bmatrix} \quad (12)$$

where $A_{in} = g(x_i - x_n)$.

According to the principle of the Tikhonov regularization in [10], [11], [25], (10) can be rewritten as an operator form,

$$\boldsymbol{A}I = \int_{-L}^{L} g(x-x')I(x')\,\mathrm{d}x' \quad (13)$$

since,

$$\boldsymbol{A}I = D \quad (14)$$

Equation (10) is ill-posed, and this property causes it to hardly be solved stably. At the same time, (14) also inherits the ill-posedness of (10), which means that when the observed data $D$ has an error, (14) is difficult to be solved correctly and stably. In order to solve this problem, according to the Appendix, a penalty is introduced into (14) as follows:

$$\alpha I^{\alpha} + \boldsymbol{A}^*\boldsymbol{A}I^{\alpha} = \boldsymbol{A}^* D^{\delta} \quad (15)$$

where $\alpha$ is the regularization parameter, the $\boldsymbol{A}^*$ represents the complex conjugate of $\boldsymbol{A}$, the $\delta$ defines the range of error between the accurate data and observed data, the $D^{\delta}$ is the observed data with error. A relationship is satisfied between the accurate and observed data.

$$\left\| D - D^{\delta} \right\| = \sqrt{\frac{1}{N+1}\sum_{i=0}^{N} \left(D_i - D_i^{\delta}\right)^2} \le \delta \quad (16)$$

When the adverse inference disappears, that is $\delta = 0$, then the $D^{\delta}$ represents accurate data and $D = D^{\delta}$.

## III. DEFINITIONS OF REGULARIZATION PARAMETER AND THE NUMBER OF DISCRETE POINTS

In this section, the main work is to determine the regularization parameter and the number of discrete points.

### A. DEFINITION OF REGULARIZATION PARAMETER

It must be noted that the selection of the regularization parameter $\alpha$ is a key step in the calculation process of the Tikhonov regularization technique. If $\alpha$ is too small, a large influence caused by perturbation error occurs in the results. However, if $\alpha$ is too large, the target results are seriously affected by excessive regularization. Therefore, the selection of a reasonable regularization parameter is an important condition for solving the target equation quickly and stably. There are many common methods for selecting regularization parameters, including L-curve method [26], Morozov deviation principle [27], generalized cross-validation criterion (GVC) [28] and Newton iterative method [29]. However, the above-mentioned methods undergo complicated calculations or multiple iterations before obtaining an appropriate regularization parameter, which is disadvantageous in terms of time occupation. Fortunately, a satisfactory result can be obtained when an initial value $\alpha_0$ of the iteration is adopted as an regularization parameter in the process of using the Newton iterative method to determine the regularization parameter. Moreover, compared with the calculation time saved by using $\alpha_0$, the small errors due to $\alpha_0$ are pleasing and fully acceptable. In the Newton iterative method, the constraint that the initial value $\alpha_0$ of iteration needs to satisfy is as follows,

$$\alpha \left( \left\| D^{\delta} \right\| - \delta \right) \leq \|\boldsymbol{A}\|^2 \delta \tag{17}$$

where $\|\cdot\|$ represents a norm. The regularization parameter can be summarized as follows,

$$\alpha \leq \frac{\|\boldsymbol{A}\|^2 \delta}{\left\| D^{\delta} \right\| - \delta} \tag{18}$$

### B. DEFINITION OF THE NUMBER OF DISCRETE POINTS

In Section II, the Simpson formula is adopted to achieve the discretization of the integral equation (7). In the process, the selection of the number $n$ of discrete points plays an important role in the fast and accurate calculation. The expression of discretization error generated by the Simpson formula is as follows [30],

$$\delta_s = -\frac{(l-0)h^4}{2880} f^{(4)}(x') \tag{19}$$

where $h = l/N$, and $f(x') = g(x - x')I(x')$.

Unfortunately, the induced current $I(x)$ which needs to be obtained is still unknown. Therefore, the fourth-order derivative $f^{(4)}(x')$ cannot be obtained. In order to overcome this difficulty, a suitable $N_0$ is defined as the initial number of discrete points. Then, the number $N$ of the optimal discrete points is obtained by increasing $N_0$ gradually according to the exponential law of $2^m$, and $m = 1, 2, 3, \cdots$. Before the optimal $N$ that satisfies (19) is obtained, the calculated induced current $I(x)$ is jagged and there are big differences between adjacent values, as shown in Fig. 2. By choosing the two induced current values with the largest difference for the adjacent positions, we assume that the optimal $n$ is obtained

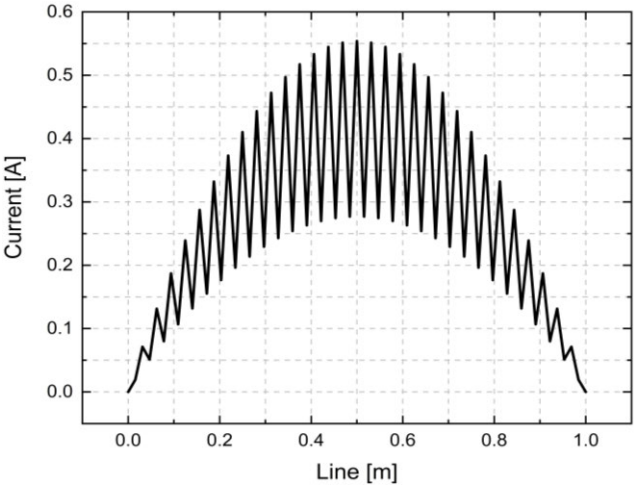


**FIGURE 2.** The HF induced current along the TL is jagged.

if the ratio of that difference to the smaller current value satisfies a certain condition. This condition can be expressed as follows

$$\frac{|I(i+1) - I(i)|}{\min\left(|I(i)|, |I(i+1)|\right)} < \varepsilon \tag{20}$$

where $\varepsilon$ is a small amount and is related to the required calculation accuracy. The flowchart of solving the optimal number $N$ of the discrete points is shown in Fig. 3.

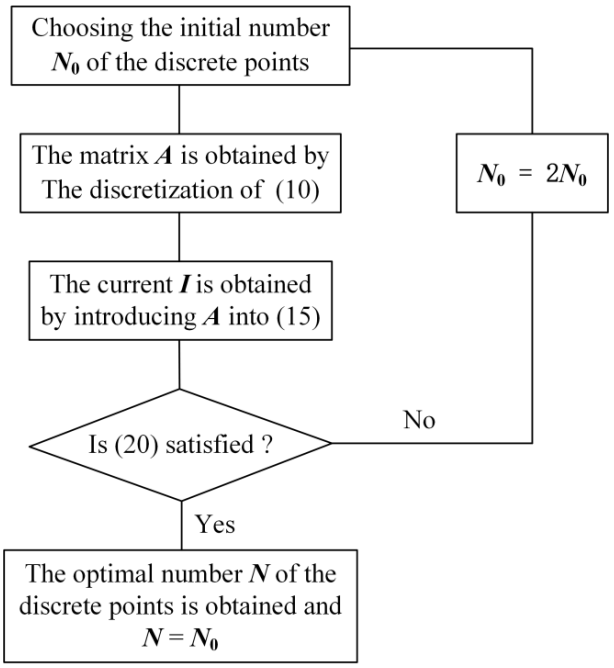


**FIGURE 3.** Flowchart of solving the optimal number $N$ of the discrete points.

## IV. NUMERICAL EXAMPLES

In this section, the TL with different configurations are selected to verify the proposed method (Tikhonov regularization technique), including the single-conductor transmission line (STL) and an MTL. All presented analyses are

performed in the frequency domain. The time-domain results are obtained by way of IFFT. At a single frequency point, for any type of the incident HFEM wave signal, only the amplitude of the induced current on the TL is affected and the law of response of the TL to the corresponding frequency is fixed. Therefore, in order to simplify the analysis process, we define the electric field strength of the incident EM wave is 1V/m at any frequency point. If the analysis of a specific signal needs to be performed, it is only necessary to change the value of the electric field strength at the corresponding frequency.

### A. OVERHEAD STL

Two different situations are examined for overhead TLs. One is a TL located inside or between the devices and the TL can be characterized by shorter length and lower height. The other is the outdoor long-distance overhead line, such as a high-voltage power TL.

#### 1) EXAMPLE 1

In Fig. 1, the dimensions of the STL with the open-circuit terminal condition at both ends are: the length $l = 1$m, the height $h = 0.1$m, the radius $r = 0.0025$m. The propagation direction of the EM waves is defined with the pitch angle $\phi = 60°$, azimuth angle $\gamma = 0°$, and polarization angle $\theta = 0°$.

In order to better compare the difference between the proposed method and Landweber iteration regularization technique (LIRT), the same discrete rule for processing the kernel function is adopted in the analysis process of the two methods.

In Fig. 4, at different frequencies, the results obtained by the proposed method and Method of Moment (MoM) are in a good agreement. The results achieved by the LIRT also agree well with MoM at 100 MHz and 500 MHz. However, the accuracy of the proposed method is obviously higher than the LIRT when the frequency rises up to 1 GHz. It is also noted that the results obtained by the proposed method are superior to the LIRT at the frequency $f = 300$ MHz. For the TL in *example 1*, $f = 300$ MHz is exactly its resonating frequency. Thus, the effectiveness of the regularization technique at the resonating frequency is indicated by the results displayed in Fig. 4b.

The information of the computation time spent by the three methods at different frequencies is listed in Table 1. It is obvious that the regularization technique can greatly reduce the computation time compared with the MoM. Relative to the MoM, only 1/8 of the computation time is spent by the LIRT, while only 1/90 of the computation time is occupied by the proposed method. This fact shows that the regularization technique has great advantages compared to the MoM at the analysis of the single-frequency point. It may be also mentioned that the computation time spent is not fixed and unique. It depends as well on the quality of the program, the configuration and operating state of the computer.

**TABLE 1. Computation time comparison between the proposed method, lirt, and MoM in Fig. 4.**

| | MoM | LIRT | The Proposed Method |
|---|---|---|---|
| 100 MHz | 9.46 s | 1.131 s | 0.101 s |
| 300 MHz | 9.57 s | 1.385 s | 0.103 s |
| 500 MHz | 9.42 s | 1.229 s | 0.098 s |
| 1 GHz | 8.35 s | 1.447 s | 0.095 s |

The results of the HFEM response of the TL are shown in Fig. 5 when the pitch angle $\phi$ changes from 15 to 90 degrees (the angles $\gamma$ and $\theta$ are kept as zero). A good agreement is achieved between the proposed method and MoM. For the

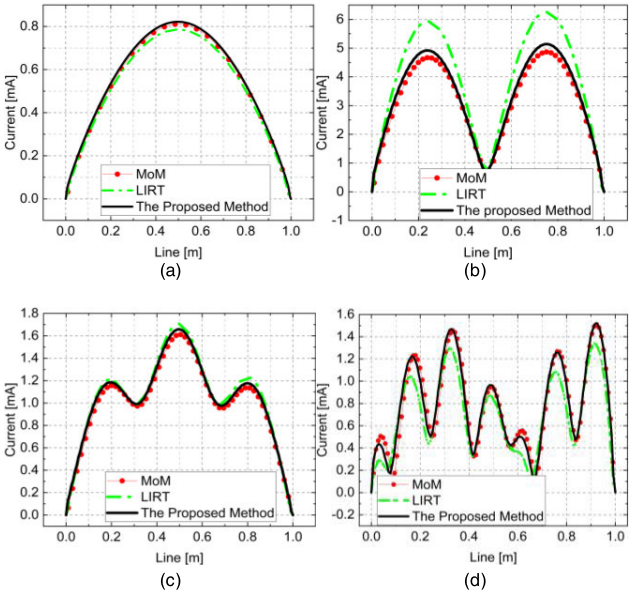


**FIGURE 4. HFEM response of the TL excited by EM waves with different frequencies. (a) $f = 100$ MHz, (b) $f = 300$ MHz, (c) $f = 500$ MHz, (d) $f = 1$ GHz.**

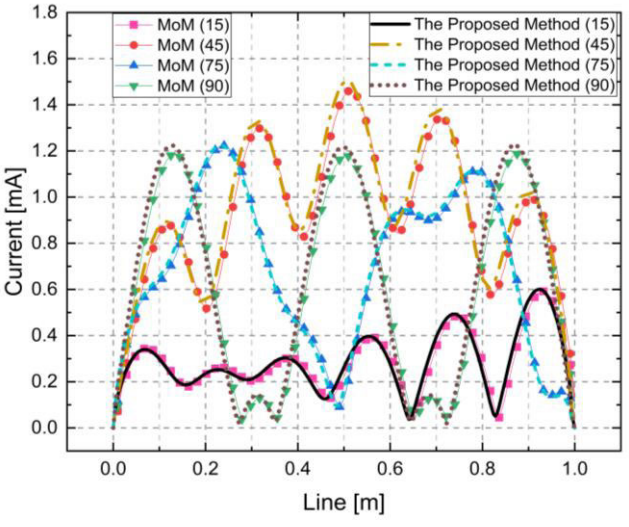


**FIGURE 5. Results of the HFEM response of the TL at different incident angles.**

comparison in Fig. 5, the change of the HFEM response of the TL illuminated by the EM waves does not show a positive or negative correlation, but presents a relatively "willful" change trend, as the change of the incident angle.

The above results are obtained with the assumption that the electric field intensity of the incident plane wave is 1 V/m. In order to observe the advantages of the proposed method more intuitively, a double exponential electromagnetic pulse (EMP) is chosen to study the EM response of the TL in time-domain. The time-domain and frequency-domain expressions of this signal are as follow,

$$E(t) = E_0\left(\mathrm{e}^{-\alpha t} - \mathrm{e}^{-\beta t}\right) \tag{21}$$

$$E(f) = E_0\left(\frac{1}{\alpha + j2\pi f} - \frac{1}{\beta + j2\pi f}\right) \tag{22}$$

where $E_0 = 1.3$ V/m, $\alpha = 4e7$, $\beta = 6e8$.

The spectrum of the HFEM response at the center of the TL is shown in Fig. 6. The time-domain results in Fig. 7 are obtained by the IFFT. It can be seen that the results obtained by the proposed method agree well with that by the MoM.

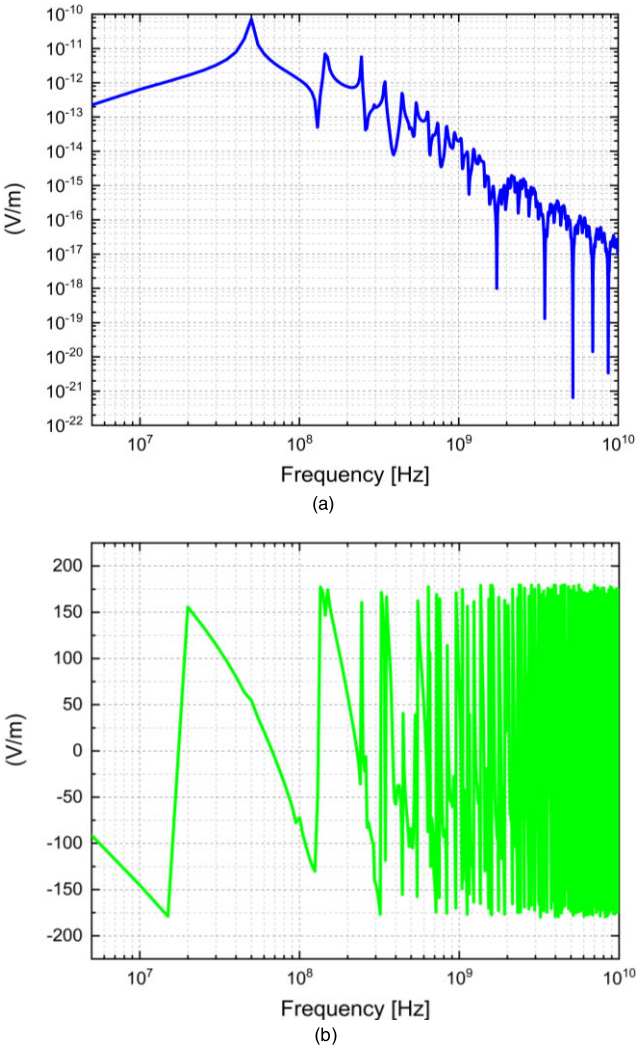


**FIGURE 6.** Spectrum of the HFEM response at the center of the TL.

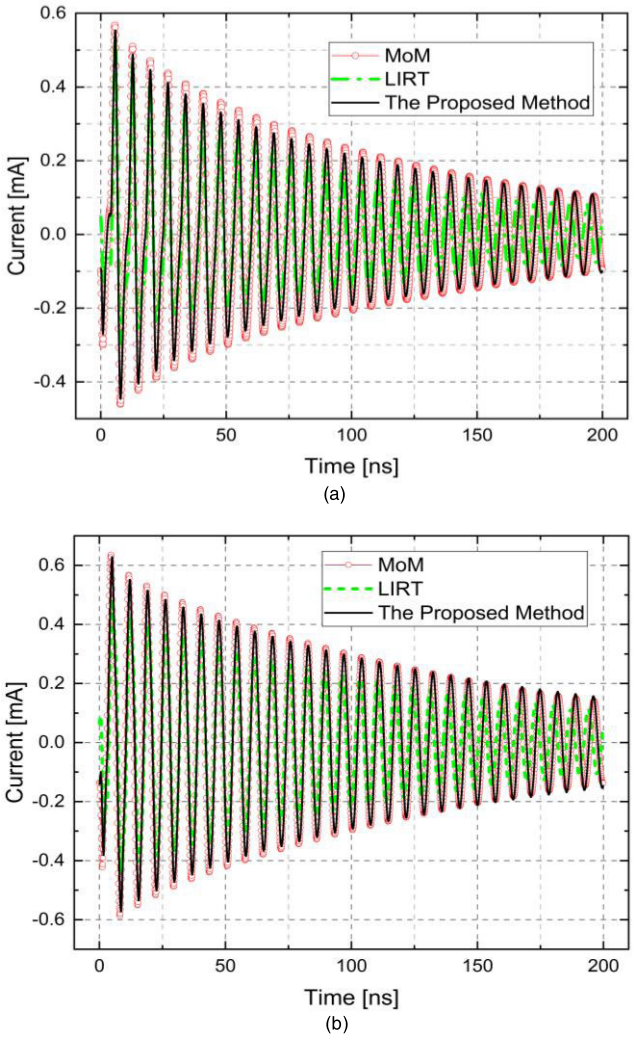


**FIGURE 7.** Time-domain HFEM response results at the center and one-quarter of the TL. (a) The time-domain waveform at the center of the TL, (b) The time-domain waveform at the one-quarter of the TL.

A more obvious error is made by the LIRT under the same discrete rule. Meanwhile, compared with the LIRT and MoM, the high-efficiency of the proposed method in terms of time occupancy is demonstrated in Table 2.

**TABLE 2.** Computation time comparison between the proposed method, lirt, and MoM in Fig. 7.

| | MoM | LIRT | The Proposed Method |
|---|---|---|---|
| Time | 353.70 s | 149.838 s | 20.761 s |

Fortunately, the fact that the computation time of the LIRT is large can be predicted. In this method, the regularization parameter ($\alpha$) and the number of iterations ($M$) are determined by the double integral of the kernel function [11]. The details are as follow,

$$\|\boldsymbol{A}\|^2 = \iint_{\Omega_L} |g(x-y)|^2 \,\mathrm{d}x\,\mathrm{d}y \tag{23}$$

where the integration interval is $\Omega_L : ([-L, L] \times [-L, L])$.

The regularization parameter is obtained by $\alpha \in (0, 2/\|\boldsymbol{A}\|^2)$. The number of iterations is the reciprocal of $\alpha$, and $M = 1/\alpha$.

When the range of the integration interval and the number of discrete points are large, a certain amount of time is spent to determine the regularization parameter and number of iterations. In general, the penalty (explained in appendix) is a minor change to the original equation, so the regularization parameter is a small value. Small $\alpha$ produces a great number of iterations, which causes a large amount of calculation time. Compared with LIRT, the most time-consuming operation of the proposed method during the calculation process is the determination of regularization parameters $\alpha$. However, this process has been properly avoided in this paper, so as to reduce the time.

#### 2) EXAMPLE 2

In Example 2, the effectiveness of the proposed method is analyzed by STL with different dimension combinations. Since the proposed method and LIRT have been described and compared in detail through Example 1, the reason why the proposed method is more efficient is investigated. Therefore, only the results obtained by the proposed method and MoM are provided in the following figures. It should be noted that the transmission line dimension in *Example 2* is larger and the incident frequency is lower compared to *Example 1*, so that the results obtained by the classical TL theory can be also possibly provided as a comparison.

For different dimension combinations in Fig. 8, it can be clearly seen that the results obtained by the proposed method agree very well with those by the MoM. Moreover, the results also are in a good agreement when the length of the STL reaches 100 m or even 200 m and the height is 10 m.

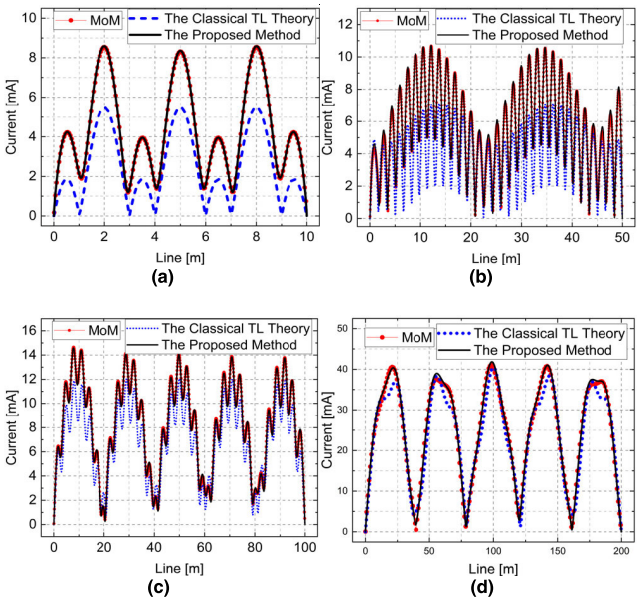


**FIGURE 8.** Induced current of the STL with Different Configuration excited by EM waves with different frequencies and angles. (a) $l = 10$ m, $h = 5$ m, $r = 0.005$ m, $f = 100$ MHz, $\gamma = 0°$, $\theta = 0°$, $\phi = 90°$. (b) $l = 50$ m, $h = 10$ m, $r = 0.005$, $f = 100$ MHz, $\gamma = 0°$, $\theta = 0°$, $\phi = 30°$. (c) $l = 100$ m, $h = 10$ m, $r = 0.005$ m, $f = 50$ MHz, $\gamma = 0°$, $\theta = 0°$, $\gamma = 45°$. (d) $l = 200$ m, $h = 10$ m, $r = 0.005$ m, $f = 10$ MHz, $\gamma = 0°$, $\theta = 0°$, $\phi = 75°$.

Therefore, the proposed method is a very effective way for analyzing the HFEM response of the large-scale overhead line (for example, power line) irradiated by strong EMP (for example, nuclear electromagnetic pulse or lightning electromagnetic pulse).

For the classical TL theory, it can not obtain an accurate result to reflect the response of the STL to the EM waves when the frequency is greater than 10 MHz, as shown in Figs. 8a, 8b, and 8c. In Fig. 8d, the result obtained by the classical TL theory is very close to that by the MoM, which indicates that the antenna mode component of the induced current is very weak already for the STL dimensions in Fig.8d and the result obtained by the classical TL theory (transmission line mode component) can be adopted to analyze the response of the field-to-line.

It is also seen from Table 3 that the proposed method can greatly reduce the computation time compared with the MoM for the STL in *Example 2*.

**TABLE 3.** Computation time comparison between the proposed method and MoM in Fig. 8.

| | MoM | The Proposed Method |
|---|---|---|
| Fig. 8a | 21.25 s | 4.541 s |
| Fig. 8b | 44.04 s | 10.605 s |
| Fig. 8c | 145.63 s | 25.321 s |
| Fig. 8d | 530.55 s | 26.034 s |

### B. OVERHEAD MTLS

#### 1) ANALYSIS OF THR HIGH-FREQUENCY MTL EQUATION

When the distance between adjacent transmission lines is so small that mutual interference cannot be ignored, the multiple TLs can be regarded as an MTL system, as shown in Fig. 9. In this case, (5) can be written in the matrix form as follows,

$$\left(\frac{\mathrm{d}^2}{\mathrm{d}\,z^2} + k^2\right) \int_{-L}^{L} \boldsymbol{G}(x|x', y|y', z|z')\boldsymbol{I}(x')\,\mathrm{d}\,x' = -\frac{4\pi k^2}{j\omega\mu_0}\boldsymbol{E}^{\mathrm{inc}}(x, y, z) \quad (24)$$

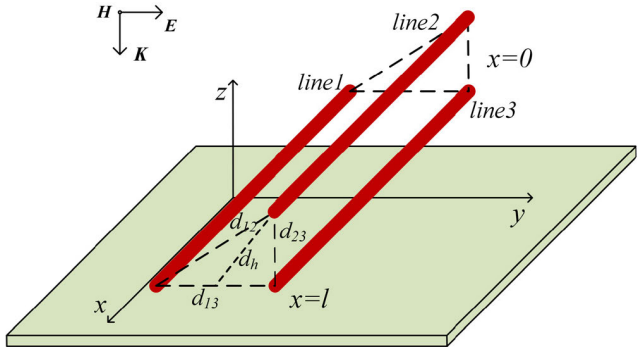


**FIGURE 9.** An overhead three-conductor TLs system irradiated by the EM plane waves.

In the matrix $\boldsymbol{G}(x|x', y|y', z|z')$, the diagonal elements define the influence between each TL itself and the corresponding mirror image, while the remaining elements represent the effects between the different lines

$$\boldsymbol{G}(x|x', y|y', z|z') = \begin{bmatrix} g_{11} & g_{12} & \cdots & g_{1N} \\ g_{21} & g_{22} & \cdots & g_{2N} \\ \cdots & \cdots & \cdots & \cdots \\ g_{N1} & g_{N2} & \cdots & g_{NN} \end{bmatrix} \tag{25}$$

where $g_{in} = g(x_i|x_n, y_i|y_n, z_i|z_n)$. The elements on the diagonal can be solved according to (6) and the remaining elements have the following relationship,

$$g_{i,n} = \frac{\mathrm{e}^{-jk\sqrt{R^2_{i,n}}}}{\sqrt{R^2_{i,n}}} - \frac{\mathrm{e}^{-jk\sqrt{R^2_{i,n\_im}}}}{\sqrt{R^2_{i,n\_im}}} \tag{26}$$

where $R^2_{i,n}$ indicates the distance between the cable to be analyzed and the other TLs.

$$R^2_{i,n} = (x_i - x_n)^2 + (\mathrm{y}_i - y_n)^2 + (z_i - z_n)^2 \tag{27}$$

and $R^2_{i,n\_im}$ defines the distance between the studied cable and the mirror image of other TLs.

$$R^2_{i,n\_im} = (x_i - x_n)^2 + (\mathrm{y}_i - y_n)^2 + (z_i - z_{n\_im})^2 \tag{28}$$

The induced current $\boldsymbol{I}(x')$ and incident electric field $\boldsymbol{E}^{\mathrm{inc}}(x, y, z)$ matrices can be expressed as follow,

$$\boldsymbol{I}(x') = \begin{bmatrix} I(x'_1) \\ I(x'_2) \\ \cdots \\ I(x'_N) \end{bmatrix} \tag{29}$$

$$\boldsymbol{E}^{\mathrm{inc}}(x, y, z) = \begin{bmatrix} E^{\mathrm{inc}}(x_1, y_1, z_1) \\ E^{\mathrm{inc}}(x_2, y_2, z_2) \\ \cdots \\ E^{\mathrm{inc}}(x_N, y_N, z_N) \end{bmatrix} \tag{30}$$

The analytic process for solving (24) is similar to the STL, and each element in $\boldsymbol{G}(x|x', y|y', z|z')$ needs to be discretized by the Simpson formula.

In particular, for the MTLs system, the matrix of the regularization parameter $\boldsymbol{\alpha}$ is a diagonal matrix whose size is determined by the numbers of the TL and discrete points in the MTLs system. For a three-conductor TL system, if each line is discretized into $N$ segments, the regularization parameter matrix becomes as follows,

$$\boldsymbol{\alpha} = \begin{bmatrix} \alpha_1 & 0 & 0 & & & & & & \\ 0 & \ddots & 0 & & \boldsymbol{0} & & & \boldsymbol{0} & \\ 0 & 0 & \alpha_1 & & & & & & \\ & & & \alpha_2 & 0 & 0 & & & \\ & \boldsymbol{0} & & 0 & \ddots & 0 & & \boldsymbol{0} & \\ & & & 0 & 0 & \alpha_2 & & & \\ & & & & & & \alpha_3 & 0 & 0 \\ & \boldsymbol{0} & & & \boldsymbol{0} & & 0 & \ddots & 0 \\ & & & & & & 0 & 0 & \alpha_3 \end{bmatrix} \tag{31}$$

where $\boldsymbol{\alpha}$ is a matrix of $3N \times 3N$.

### 2) NUMERICAL EXAMPLE

In this verification, the application of the proposed method in analyzing the HFEM response problem of the MTLs system with open-circuit conditions illuminated by EM waves is shown. The regularization parameters of various lines with different configurations in the MTLs system are not identical, which means the required number of iterations is different when the LIRT is used to accurately calculate the induced current on each line. This fact makes it difficult for the LIRT to be conveniently applied in the analysis of HFEM response problem of the MTLs system. Therefore, only the results obtained by the proposed method and the MoM are provided in the following result figures.

In order to simplify the analysis process, we assume that the configurations (including the parameter configurations of the TL and the spatial position of the TL) of lines 1 and 3 are the same in Fig. 9. Therefore, in the following comparison figures, only the induced currents on lines 1 and 2 are shown. In Fig. 9, $d_h$ defines the difference in horizontal height between line 2 and lines 1 or 3, and $d_h = h_2 - h_{1,3}$. $d_{12}$, $d_{13}$ and $d_{23}$ are the distances between three lines, respectively

#### *a: MTLS 1*

In this verification, an overhead three-conductor TL system is studied, as shown in Fig. 9. The lengths of all the three lines are $l = 10$ m. The heights are $h_1 = h_3 = 1$ m, and $h_2 = 1.1$ m, respectively. The radii are $r_1 = r_2 = r_3 = 0.0025$m. The frequency $f = 100$MHz, the pitch angle $\phi = 75°$, azimuth angle $\gamma = 0°$, and polarization angle $\theta = 0°$.

In order to more clearly show the mutual-influence between the various lines in the MTLs system, the results of the HFEM response of each line in the MTLs system that is considered as an STL are analyzed separately in this verification.

In Fig. 10, the difference between the results of STL and the results obtained by the proposed method and MoM indicates that the mutual interference between the various lines in the MTLs system is not negligible. Therefore, it is necessary to study all the STLs as a whole when analyzing the EM response of each line in the MTLs system. If the mutual interference is ignored and a STL in the MTLs system is analyzed

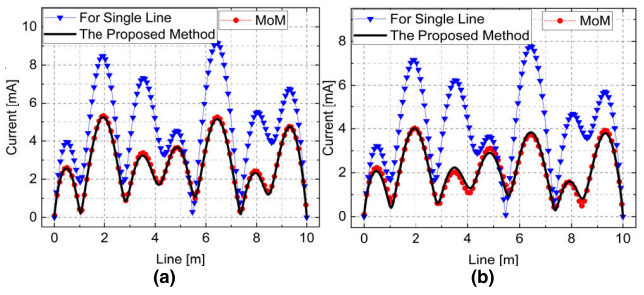


**FIGURE 10.** Comparison of the results obtained by the proposed method, MoM, and STL on lines 1 and 2. (a) the results on the line1, (b) the results on the line2.

independently, it is difficult to obtain the correct result. This operation is reasonable when the distance between lines in the MTL system is sufficiently far away so that the mutual interference can be completely ignored. Moreover, a good agreement is achieved between the proposed method and MoM, which indicates that the proposed method is also effective for analyzing the HFEM response of the MTLs.

The comparison of the computation time between the proposed method and MoM is shown in Table 4. The proposed method has obvious advantages compared with MoM for analyzing the HFEM response of the MTLs system. In this verification, the proposed method can reduce the spent time by about 80%. It should be noted that the computation time of the STL is not given, because the STL case and the other two methods can not be regarded as the analysis of the same model.

**TABLE 4. Computation time comparison between the proposed method and MoM in Figs. 10 and 11.**

| | MoM | The Proposed Method |
|---|---|---|
| Fig. 10a, b | 23.45 s | 7.28 s |
| Fig. 11a, b | 11.90 s | 1.085 s |
| Fig. 11c, d | 13.67 s | 1.145 s |

*b: MTLS 2*

In this verification, the lengths of three lines all are $l = 4$m. The heights are $h_1 = h_3 = 0.5$ m, and $h_2 = 0.55$ m, respectively. The radii are $r_1 = r_2 = r_3 = 0.0025$m. The azimuth angle $\gamma = 0°$, and polarization angle $\theta = 0°$.

The HFEM response results of the MTLs system illuminated by the incident EM waves with two different parameters (200 MHz and 30 degrees, 100 MHz and 75 degrees) are shown in Fig. 11. The results for different lines of the MTLs system obtained by the proposed method and MoM are in a very good agreement. Moreover, the efficiency of the proposed method is clearly reflected by the time information in Table 4. The proposed method takes only about 1/10 of the time consumed by the MoM under the same conditions.

### 3) ANALYSIS OF DIFFERENT LEVELS OF ERROR

The accuracy of an ill-posed problem analyzed via the regularization technique is affected by factors, including the number of discrete points, the form of the kernel function, the value of the regularization parameter, and the error levels of the observed data. In the above analysis, the effects of discrete points and regularization parameters are already analyzed, and the form of the kernel function is fixed for the research object. Therefore, only the error level of the observed data is analyzed in this part with the pitch angle $\phi = 90°$, azimuth angle $\gamma = 0°$, and polarization angle $\theta = 0°$.

An STL is selected as the research object, and its length is $l = 3$m, height is $h = 0.5$m, radius is $r = 0.005$m. According the phenomenon in the results figure, the accuracy

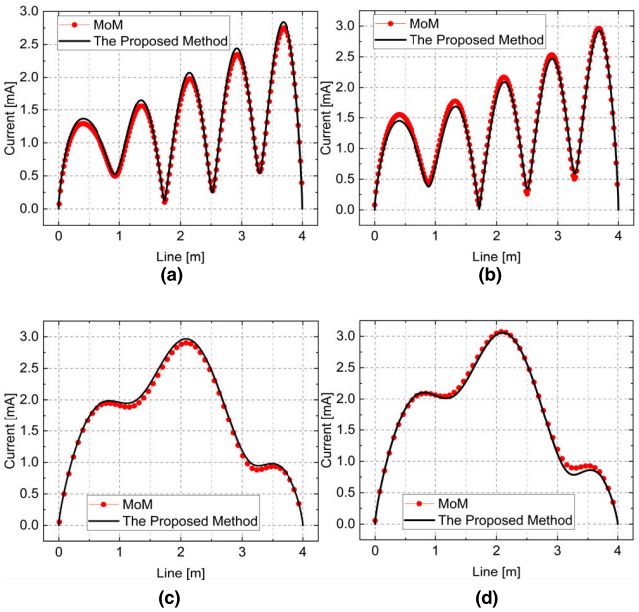


**FIGURE 11. Comparison of the HFEM response on the MTLs system excited by the EM waves with different frequencies and angles of incident. (a) $f = 200$ MHz, $\phi = 30°$, the results on the line 1. (b) $f = 200$ MHz, $\phi = 30°$, the results on the line 2. (c) $f = 100$ MHz, $\phi = 75°$, the results on the line 1. (d) $f = 100$ MHz, $\phi = 75°$, the results on the line 2.**

of the proposed method decreases accordingly as the error increases. Moreover, different functions respond differently to changes in error. Fig. 12 illustrates that the studied equation is sensitive to changes in error. When the error level of the observed data reaches 5%, there is already an error that cannot be ignored in the results.

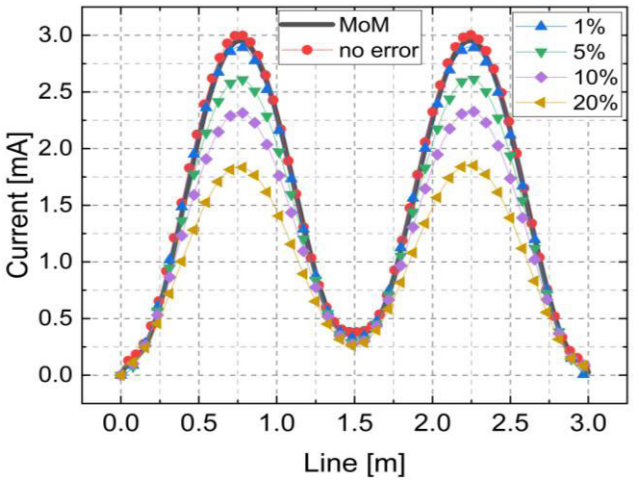


**FIGURE 12. Calculation results of the proposed method in different levels of error.**

According to (5), a predictable phenomenon that the accuracy of the proposed method is different for the TLs with different configurations at the same error. In order to verify this speculation, an STL with different heights has been investigated. The length of the STL is $l = 3$m, the radius

is $r = 0.005$m, the height is $h = 0.1$m, 0.5m and 1m, respectively. The frequency of the incident EM waves is $f = 200$MHz.

In Fig. 13, the absolute error and relative error between the results obtained via the accurate data of electric field and the observed data with a 5% error are shown, and our expectation is proved by this result. It is noteworthy that the values of absolute error near the terminals of the STL are small, while the relative error is very large, which is a normal phenomenon. The values of the induced current at the terminals of the TL with open-circuit condition should be equal to zero, so a large relative error could be caused by a small absolute error.

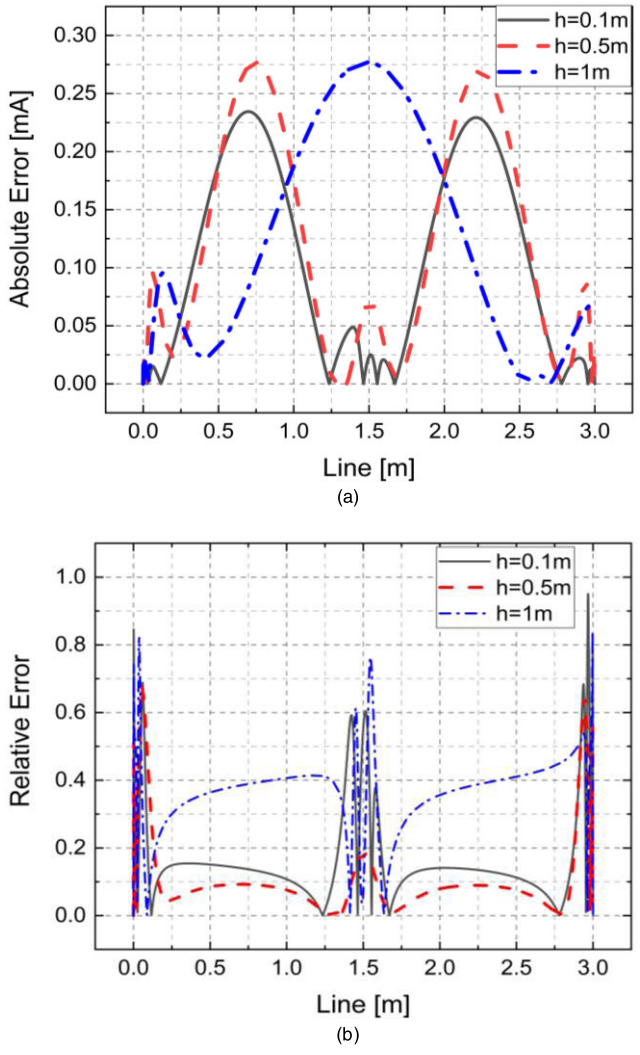


**FIGURE 13.** Results of the absolute and relative errors. (a) Absolute error, (b) Relative error.

## V. CONCLUSION

The HFEM response of a TL irradiated by EM waves can be expressed by solving the general TL model. In this model, the most difficult part is the process of the Fredholm integral equation of the first kind with ill-posedness. Fortunately, the regularization technique is a mature method for dealing with the ill-posed problem. Therefore, in this paper, the application of the Tikhonov regularization technique for analyzing the HFEM response of a TL irradiated by EM waves has been studied. In order to save computation time and obtain results with sufficient accuracy, the iterative initial value of the Newton iteration method has been adopted as a regularization parameter. Moreover, a suitable method for determining the number of discrete points has been found by analysis. The effectiveness of the proposed method has been verified by different numerical examples including the STLs with different configurations as well as the MTLs system. Finally, for different levels of error, the applicability of the proposed method has been also analyzed.

The proposed method is defective for the analysis of the HFEM response of a MTLs system. We can reasonably speculate that the definition of the regularization parameter matrix is an important factor leading to this shortcoming. Therefore, finding a suitable method for defining the regularization parameter matrix of the MTLs system is one of the focus of our next work.

For the actual TL with loads, a perfect way to analyze its HF response is hardly seen yet. Of course, the methods in [5], [12]–[14] are useful for a transmission line with loads, and certain limitations also present. However, it would be interesting to find some possible combination between these methods and regularization.

## APPENDIX

Mathematical details of the Tikhonov regularization technique are provided in this section.

In the finite space, the least-squares solution represents an approximate solution to a set of linear algebraic equations $\boldsymbol{H}x = y$, that is to say, the continuous functional is minimized in the finite space $X$. If $\boldsymbol{H}$ is tight and $X$ is infinite, the minimization problem is ill-posed and the value of $x$ cannot be solved steadily.

We assume that $X$ and $Y$ are Hilbert spaces, $\boldsymbol{H} : X \to Y$ is bounded linear operator, and $\hat{x}$ is the approximation of $x$. For $y \in Y$, in the case that $\hat{x} \in X$, an expression can be written as follows,

$$\left\|\boldsymbol{H}\hat{x} - y\right\| \leq \|\boldsymbol{H}x - y\| \tag{32}$$

The condition that (27) holds for all $\hat{x}$ is,

$$\boldsymbol{H}^*\boldsymbol{H}\hat{x} = \boldsymbol{H}^*y \tag{33}$$

where $\boldsymbol{H}^* : Y \to X$ is the adjoint operator of $\boldsymbol{H}$.

The analysis of X can be replaced by solving (33). However, whether the equation has a unique and stable solution is uncertain, because the minimization problem is ill-posed. In order to ensure the uniqueness of the minimal element $\hat{x}$, a limit must be adopted for $\hat{x}$. Therefore, a penalty $\alpha\hat{x}$ must be added to the objective function $\|\boldsymbol{H}x - y\|$ to make the equation a well-posed equation.

$$\boldsymbol{H}^*\boldsymbol{H}\hat{x} + \alpha\hat{x} = \boldsymbol{H}^*y \tag{34}$$

where $\alpha$ represents the regularization parameter.

## REFERENCES

[1] C. R. Paul, *Analysis of Multiconductor Transmission Lines*. New York, NY, USA: Wiley, 1994.
[2] F. M. Tesche, M. V. Ianoz, and T. Karlsson, *EMC Analysis Methods and Computational Models*. New York, NY, USA: Wiley, 1997.
[3] F. M. Tesche, "Development and use of the BLT equation in the time domain as applied to a coaxial cable," *IEEE Trans. Electromagn. Compat.*, vol. 49, no. 1, pp. 3–11, Feb. 2007.
[4] L. Xie and Y.-Z. Lei, "Transient response of a multiconductor transmission line with nonlinear terminations excited by an electric dipole," *IEEE Trans. Electromagn. Compat.*, vol. 51, no. 3, pp. 805–810, Aug. 2009.
[5] F. Rachidi and S. Tkachenko, *Electromagnetic Field Interaction With Transmission Lines: From Classical Theory to HF Radiation Effects*. Boston, MA, USA: WIT Press, 2008.
[6] S. Tkachenko, F. Rachidi, and M. Ianoz, "Electromagnetic field coupling to a line of finite length: Theory and fast iterative solutions in frequency and time domain," *IEEE Trans. Electromagn. Compat.*, vol. 37, no. 4, pp. 509–518, Nov. 1995.
[7] S. Tkachenko, F. Rachidi, and M. Ianoz, "High-frequency electromagnetic field coupling to long terminated lines," *IEEE Trans. Electromagn. Compat.*, vol. 43, no. 2, pp. 117–129, May 2001.
[8] D. Poljak, F. Rachidi, and S. Tkachenko, "Generalized form of telegrapher's equations for the electromagnetic field coupling to finite-length lines above a lossy ground," *IEEE Trans. Electromagn. Compat.*, vol. 49, no. 3, pp. 689–697, Aug. 2007.
[9] J. Nitsch and S. Tkachenko, "High-frequency multiconductor transmission-line theory," *Found. Phys.*, vol. 40, nos. 9–10, pp. 1231–1252, Oct. 2010.
[10] M. Brignone, F. Delfino, R. Procopio, M. Rossi, F. Rachidi, and S. V. Tkachenko, "An effective approach for high-frequency electromagnetic field-to-line coupling analysis based on regularization techniques," *IEEE Trans. Electromagn. Compat.*, vol. 54, no. 6, pp. 1289–1297, Dec. 2012.
[11] M. Brignone, F. Delfino, R. Procopio, and M. Rossi, "An equivalent two-port model for a transmission line of finite length accounting for high-frequency effects," *IEEE Trans. Electromagn. Compat.*, vol. 56, no. 6, pp. 1657–1665, Dec. 2014.
[12] H. Haase and J. Nitsch, "Full-wave transmission line theory (FWTLT) for the analysis of three-dimensional wire-like structures," in *Proc. 14th Int. Zurich Symp. Tech. Exhib. Electromagn. Compat.*, Zürich, Switzerland, Feb. 2001, pp. 235–240.
[13] H. Haase, J. Nitsch, and T. Steinmetz, "Transmission-line super theory: A new approach to an effective calculation of electromagnetic interaction," *Radio Sci. Bull.*, vol. 2003, no. 307, pp. 33–60, Dec. 2003.
[14] H. Haase, T. Steinmetz, and J. Nitsch, "New propagation models for electromagnetic waves along uniform and nonuniform cables," *IEEE Trans. Electromagn. Compat.*, vol. 46, no. 3, pp. 345–352, Aug. 2004.
[15] J. Nitsch, F. Gronwald, and G. Wollenberg, *Radiating Nonuniform Transmission-Line Systems and the Partial Element Equivalent Circuit Method*. New York, NY, USA: Wiley, 2009.
[16] R. Rambousky, J. B. Nitsch, and H. Garbe, "Application of the transmission line super theory to multiwire TEM-waveguide structures," *IEEE Trans. Electromagn. Compat.*, vol. 55, no. 6, pp. 1311–1318, Dec. 2013.
[17] A. Maffucci, G. Miano, and F. Villone, "An enhanced transmission line model for conducting wires," *IEEE Trans. Electromagn. Compat.*, vol. 46, no. 4, pp. 512–528, Nov. 2004.
[18] L. Landweber, "An iteration formula for Fredholm integral equations of the first kind," *Amer. J. Math.*, vol. 73, no. 3, pp. 615–624, Jul. 1951.
[19] J. Yu, F. Liu, J. Wu, L. Jiao, and X. He, "Fast source reconstruction for bioluminescence tomography based on sparse regularization," *IEEE Trans. Biomed. Eng.*, vol. 57, no. 10, pp. 2583–2586, Oct. 2010.
[20] M. Wu, J. Sun, J. Zhou, and G. Xue, "Color constancy based on texture pyramid matching and regularized local regression," *J. Opt. Soc. Amer. A, Opt. Image Sci.*, vol. 27, no. 10, pp. 2097–2105, Oct. 2010.
[21] W. Zheng, Y. Qian, and M. Ye, "A grouped structure-based regularizedregression model for text categorization," *J. Softw.*, vol. 7, no. 9, pp. 2119–2124, Sep. 2012.
[22] L. Bar, N. Sochen, and N. Kiryati, "Semi-blind image restoration via Mumford-Shah regularization," *IEEE Trans. Image Process.*, vol. 15, no. 2, pp. 483–493, Feb. 2006.
[23] M. Soleimani, W. R. B. Lionheart, A. J. Peyton, X. Ma, and S. R. Higson, "A three-dimensional inverse finite-element method applied to experimental eddy-current imaging data," *IEEE Trans. Magn.*, vol. 42, no. 5, pp. 1560–1567, May 2006.
[24] D. Colton and R. Kress, *Inverse Acoustic and Electromagnetic Scattering Theory*. New York, NY, USA: Springer-Verlag, 1997.
[25] A. N. Tikhonov and V. Y. Arsenin, *Solutions of Ill-Posed Problems*. New York, NY, USA: Wiley, 1977.
[26] P. C. Hansen and D. P. O'Leary, "The use of the L-curve in the regularization of discrete ill-posed problems," *SIAM J. Sci. Comput.*, vol. 14, no. 6, pp. 1487–1503, Nov. 1993.
[27] V. A. Morozov, *Methods for Solving Incorrectly Posed Problems*. New York, NY, USA: Springer, 1984.
[28] J. M. Bardsley and J. Goldes, "Regularization parameter selection methods for ill-posed Poisson maximum likelihood estimation," *Inverse Problems*, vol. 25, no. 8, pp. 1–8, Aug. 2009.
[29] M. K. Ng, L. Qi, Y.-F. Yang, and Y.-M. Huang, "On semismooth Newton's methods for total variation minimization," *J. Math. Imag.*, vol. 27, no. 3, pp. 265–276, Apr. 2007.
[30] K. E. Atkinson, *Theoretical Numerical Analysis: A Functional Analysis Framework*. New York, NY, USA: Springer, 2000.

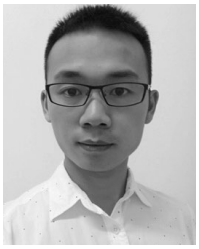

**YIN ZHANG** was born in Zunyi, Guizhou, China, in 1994. He received the B.S. degree in electronic information science and technology from Southwest Jiaotong University, Chengdu, China, in 2017, where he is currently pursuing the Ph.D. degree.

His research interests include electromagnetic compatibility and transmission line analysis.

**CHENG LIAO** was born in Chongqing, China, in 1964. He received the Ph.D. degree in electromagnetic fields and microwave techniques from the University of Electronic Science and Technology of China, Chengdu, China, in 1995.

From 1997 to 1998, he was a Visiting Scholar with the City University of Hong Kong, Hong Kong. In 1998, he became a Professor with Southwest Jiaotong University, Chengdu. His research interests include computational electromagnetic, electromagnetic compatibility, and antenna theory and design.

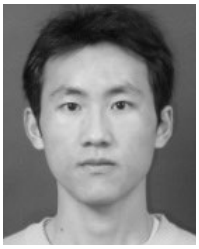

**YUPING SHANG** received the B.Sc. degree in electronic information science and technology from the Sichuan University of Science and Engineering, Zigong, China, in 2009, and the Ph.D. degree in radio physics from the University of Electronic Science and Technology of China, Chengdu, China, in 2015.

From 2015 to 2017, he was with Nanyang Technological University, Singapore, as a Postdoctoral Research Fellow. He is currently with Southwest Jiaotong University, Chengdu. His research interests include radar cross-section control and analysis, as well as antenna element and array.

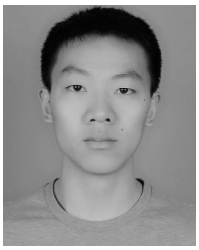

**WEI DU** was born in Nanchong, Sichuan, China, in 1993. He received the B.S. degree in electronic information science and technology from Southwest Jiaotong University, Chengdu, China, in 2017, where he is currently pursuing the Ph.D. degree.

His research interests include electromagnetic compatibility and microstrip line coupling analysis.

**RUI HUAN** was born in Yichang, Hubei, China, in 1992. He received the B.S. degree in electronic information science and technology from Southwest Jiaotong University, in 2014, where he is currently pursuing the Ph.D. degree.

His research interests include electromagnetic compatibility, transmission line analysis, and computational electromagnetics.